Published in final edited form as:
Mamm Genome. 2007 August ; 18(8): 584–595. doi:10.1007/s00335-007-9036-2.

Testicular germ cell tumor susceptibility genes from the consomic 129.MOLF-Chr19 mouse strain

Rui Zhu and **Angabin Matin**
Department of Cancer Genetics, The University of Texas M.D. Anderson Cancer Center, 1515 Holcombe Blvd., Unit 1006, Houston, Texas 77030, USA

Yuan Ji
Department of Bioinformatics and Computational Biology, The University of Texas M.D. Anderson Cancer Center, Houston, Texas 77030, USA

Lianchun Xiao
Department of Biostatistics, The University of Texas M.D. Anderson Cancer Center, Houston, Texas 77030, USA

Abstract

Chromosome substitution strains (CSS or consomic strains) are useful for mapping phenotypes to chromosomes. However, huge efforts are needed to identify the gene(s) responsible for the phenotype in the complex context of the chromosome. Here we report the identification of candidate disease genes from a CSS by using a combination of genetic and genomic approaches and by using knowledge about the germ cell tumor disease etiology. We used the CSS 129.MOLF-Chr19 chromosome substitution strain, in which males develop germ cell tumors of the testes at an extremely high rate. We were able to identify three protein-coding genes and one microRNA on chromosome 19 that have previously not been implicated to be testicular tumor susceptibility genes. Our findings suggest that changes in gene expression levels in the gonadal tissues of multiple genes from Chr 19 likely contribute to the high testicular germ cell tumor (TGCT) incidence of the 129.MOLF-Chr19 strain. Our data advance the use of CSS to identify disease susceptibility genes and demonstrate that the 129.MOLF-Chr19 strain serves as a useful model to elucidate the genetics and biology of germ cell transformation and tumor development.

Introduction

Testicular germ cell tumors (TGCTs or testicular cancers) in humans occur in males of all age groups but the most common form develops in young males between the ages of 15 and 45 years (Ilson et al. 1991). The various forms of TGCTs differ in terms of age of onset, tissue histology, and degree of malignancy. However, most germ cell tumors in humans and mice share two common features: the cancer cells originate from primordial germ cells (PGCs) (Dieckmann and Skakkebaek 1999; Oosterhuis and Looijenga 2005; Skakkebaek et al. 1987) and the cancerous transformation of PGCs occurs in the gonads during embryonic development (Kawakami et al. 2006; Looijenga et al. 2003; Smiraglia et al. 2002; Stevens 1966, 1967, 1970, 1973a).

e-mail: amatin@mdanderson.org.

Electronic supplementary material The online version of this article (doi: 10.1007/s00335-007-9036-2) contains supplementary material, which is available to authorized users.

There is strong evidence of genetic susceptibility to TGCTs in humans. Family history is a strong risk factor for TGCTs, as the risk among siblings is higher than for other cancers (Forman et al. 1992; Heimdal et al. 1996; Hemminki and Li 2004). TGCT development is also associated with sterility and other genitourinary defects (Harland et al. 1998; Jacobsen et al. 2000; Rapley et al. 2000; Tollerud et al. 1985) and is thought to be a subset of testicular dysgenesis syndrome (Skakkebaek et al. 2003). However, to date TGCT susceptibility genes have not been positively identified in humans. Genome-wide linkage screen for TGCT susceptibility loci using 273 pedigrees with two or more cases of TGCTs failed to identify any locus with certainty, and the studies suggest that multiple susceptibility loci with weak effects contribute to TGCT development (Crockford et al. 2006).

In mice, males of the 129 inbred mouse strain are genetically predisposed to develop congenital TGCTs (Stevens and Hummel 1957), which resemble pediatric germ cell tumors or testicular type I germ cell tumors (Horwich et al. 2006; Oosterhuis and Looijenga 2005; Rescorla 1999). TGCT development in 129 mice serves as a valuable system to identify genes that initiate the processes of PGC transformation. The strains that we used in this study include the 129 and the 129.MOLF-Chr19 mouse strains. The 129 has an inherent low predisposition to develop TGCTs and 6%-10% of the males develop TGCTs. The 129.MOLF-Chr19 mouse strain (also referred to as consomic, chromosome substitution strain or CSS) (Matin et al. 1999; Youngren et al. 2003) differs from the 129 because Chr 19 of the MOLF strain replaces that of the 129. Seventy percent to 80% of the males of the 129.MOLF-Chr19 strain develop TGCTs. In this article we report on the etiology of tumor development in the 129.MOLF-Chr19. Previous work has indicated five regions (named regions I to V) on 129.MOLF-Chr19 where TGCT susceptibility loci are possibly located (Youngren et al. 2003). By creating a new congenic mouse strain, we delineated one TGCT susceptibility locus to a 7.6-Mb region in mid-Chr 19 (named locus 1). To identify TGCT susceptibility genes within this locus, we compared gene expression profiles of the gonads of the 129.MOLF-Chr19 strain (high TGCT incidence) to that of the 129 strain (low TGCT incidence). Microarray analysis identified a novel TGCT candidate gene, *D19Bwg1357e*, that maps within locus 1 and whose expression is decreased in the gonads of the 129.MOLF-Chr19 strain. Additional candidate TGCT susceptibility genes were found that map to proximal and distal mouse Chr 19. The expression levels of the genes in the gonads were validated by qRT-PCR. We also examined the microRNAs that map to Chr 19 as possible TGCT susceptibility factors and found that the expression of one microRNA, mmu-miR-107, is increased in testicular tumors. In summary, our studies have identified multiple genes that, in general, behave as hypomorphs in the 129.MOLF-Chr19 strain and may contribute to testicular germ cell tumor susceptibility of this strain.

Materials and methods

Mouse strains

The 129.MOLF-Chr19 (Matin et al. 1999), 129 (129S1/SvImJ; JR002448, Jackson Laboratory, Bar Harbor, ME) and 129;*Oct4*-GFP (Youngren et al. 2005) strains have been described. All 129-derived strains are on the 129S1/SvImJ background. Mice were maintained on a 12/12-h light/dark cycle and fed NIH-31 diet *ad libitum*.

Creation of congenic-L1

To create the congenic-L1 mouse strain, the 129.MOLF-Chr19 strain was crossed to 129 (129S1/SvImJ). Progeny were backcrossed to 129 and backcross progeny were genotyped and selected for MOLF alleles for the markers *D19Mit97* and *D19Mit57* to generate congenic-L1. Selected progeny were intercrossed to homozygose the MOLF-containing region. To verify

the boundaries of the congenic regions, progeny were genotyped with SSLP markers flanking these markers and markers spanning mouse Chr 19 (Matin et al. 1999).

Creation of 129.MOLF-Chr19; *Oct4*-GFP

This strain was made by crossing 129.MOLF-Chr19 to the 129;*Oct4*-GFP mouse line (Youngren et al. 2005). The progeny from these crosses were intercrossed and selected by genotyping to identify and breed mice homozygous for MOLF-Chr 19 (equivalent to 129.MOLF-Chr19 strain) and which also carried the *Oct4*-GFP transgene.

Microscopy

PN1 testes were isolated from male mice. The testes were observed and photographed using reflected light of the Leica MZFL111 fluorescence stereomicroscope configured with a Photometric' CoolSnap Pro color CCD camera (Roper, Tucson, AZ) and Image Pro software (Media Cybernetics, Silver Spring, MD). The same testes were then observed for GFP fluorescence using the Zeiss LSM 510 confocal microscope (excitation at 488 nm) and a transmission detector (for DIC). Vertical stacks of optical sections through the specimen were acquired and then reconstructed into 3D projections. Image stacks were deconvolved to enhance contrast and improve the signal-to-noise component. The testes were then preserved overnight in 10% phosphate-buffered formalin before sectioning and staining with hematoxylin and eosin (H&E).

Tissue collection for microarray

Pregnant females were sacrificed to isolate embryos at E13.5. To isolate genital ridges, embryos were washed in PBS (phosphate-buffered saline)/0.1% DEPC (diethyl pyrocarbonate) and dissected to isolate the genital ridges. PN1 testes were isolated after decapitation of newborn males of the 129.MOLF-Chr19 and 129 strains. All tissues isolated for RNA extraction were immersed in RNA*later* Stabilization Reagent (Qiagen, Valencia, CA) and stored at -80°C. Tissue from the limbs of each embryo was used for genotyping for Chr Y sequences (G747: 5′-AGGAATTTG CTCATTTTTCAGC-3′; G632: 5′-AGAGGCTTTGCT TTCCTTAC-3′). RNA was extracted from the tissues by repeated homogenization with a 25-gauge needle (20 gauge for embryos). Tissues were pooled and RNA was prepared by using the Qiagen RNeasy Mini Kit according to the manufacturer's instructions. The concentration of RNA extracted from the tissues was determined by spectrophotometric analysis at A260 and analysis using the Agilent 2100 Bioanlyzer (Agilent Technologies, Santa Clara, CA) for quality control.

Gene expression profiling

Microarray was performed with 5 mg total RNA using the GeneChip® Mouse Genome 430 2.0 (Affymetrix, Santa Clara, CA). Data were analyzed with the DNA-Chip analyzer (dChip) version 1.3 (Li and Wong 2001). The cRNA preparation and hybridization procedures were performed as previously described (Ju et al. 2005).

Analysis of microarray results

Data analyses included the following procedures:

(1) Data preprocessing and quality assessment—We used dChip (Li and Wong 2001) analyzer version 1.3 to estimate gene expressions and to assess the quality of the data. To adjust the brightness of the six arrays to a comparable level and minimize the systematic error, we quantile-normalized all the arrays so that they had the same 75 percentile gene expression levels. We checked the quality of each array by inspecting array images and summarization files of dChip analysis. These arrays appeared to be of good quality and did not possess major manufacturing defects or abnormalities. All six arrays were therefore included

in the subsequent analysis. Next, we removed genes with low expression or with small variation. Specifically, we removed those genes with fewer than three "Present" calls or with a standard deviation (SD) less than 0.18. As a result we arrived at 24,699 (of 45,101) probe sets. To explore data structure, we performed hierarchical clustering analysis of samples using the remaining 24,699 genes.

(2) Identifying differentially expressed genes—We obtained a fold change of each gene between the two mouse strains for each of the three tissue samples. For each tissue sample we identified genes with fold change greater than 2. Consequently, we obtained 35 genes for the tissue sample from embryos, 10 for the sample from genital ridges, and 266 for the sample from newborn testes. We cross-examined the three lists of selected genes and found three common genes. The expression level of the three common genes in the two strains was subsequently verified by qRT-PCR.

Quantitative real-time PCR

PCR was performed in an ABI PRISM 7900 Sequence Detection system (Applied Biosystems, Foster City, CA). A 20-μl reaction volume contained 37.5 ng cDNA, 0.3 μM forward and reverse primers (Integrated DNA Technologies, Coralville, IA), and SYBR Green PCR Master Mix (Applied Biosystems). Samples were run in duplicates and the experiment was repeated at least twice. The housekeeping gene glyceraldehyde-3-phosphate dehydrogenase (GAPDH) was used as control. The initial denaturation was at 95°C for 10 min followed by 40 cycles of denaturation at 95°C for 15 sec, and elongation at 60°C for 60 sec. Each PCR result was normalized against the value for GAPDH. The qRT-PCR primers for *D19Bwg1357e* and *Cox15* did not but those for *Zfp162* partially overlapped with the probe sets in the microarray GeneChip. The primer pairs used are as follows: *Cox15*: F: 5′-CACTGCTACTGCCTCAGCAC, R: 5′-TGAGAGAGCCGTGAGGAACA; *D19Bwg1357e*: F: 5′-GTGAGACTGAGTACTACACAGTATGGC, R: 5′-GCTGTCTCCTTTCCTAAATTAAGC; *Zfp162*: F: 5′-TTCTTCGTTCTGCTGCTTTGC, R: 5′-GTGAAAAGAACGCGCATTACAC.

Tumor characterization

Adult males (4–6 weeks old) of the congenic-L1 strain were sacrificed and their testes were examined for tumors. Most tumors can be detected visually at that age. Alternatively, tumors were preserved in 10% phosphate-buffered formalin for at least 48 h before sectioning (5 μm) and staining with H&E.

Sequence analysis

To compare exon sequences, PCR primers were designed to either amplify cDNA or flank putative exons by more than 30 bases on either side of the exon boundary. PCR products were generated using standard conditions, quantitated by gel electrophoresis and purified before sequencing. Sequence variations, if detected, were verified by resequencing. Gene sequences from the MOLF strain have been deposited in the NCBI dbSNP.

Detection of microRNAs

Small RNA (sRNA) samples were prepared using the *mir*Vana™ miRNA Isolation Kit (Ambion, Austin, TX). We isolated sRNA samples from adult testes (4 testes from each strain) of 129 and 129.MOLF-Chr19 strains, 129.MOLF-Chr19 testicular tumors (4 testicular tumors), PN1 testes (60 testes from each strain), and E13.5 embryos (2 embryos from each strain) from 129 and 129.MOLF-Chr19. RNase protection assays (RPA) were performed using the *mir*Vana™ miRNA probe construction and detection kits (Ambion) according to the

manufacturer's instructions; 0.1μg of sRNAs was used per reaction. DNA oligos to generate the RPA probes are given in Table 1.

Results

Etiology of TGCT development in the 129.MOLF-Chr 19 strain

To guide our efforts toward identification of TGCT-causing genes, we examined the etiology of germ cell tumor development in the 129.MOLF-Chr19 strain. The etiology of germ cell tumor development has been described in the 129 strain (Stevens and Hummel 1957). To examine TGCT development in the 129.MOLF-Chr19 strain, we introduced the transgene-carrying green fluorescent protein (GFP) driven by the germ cell-specific promoter *Oct4* (*GOF-1/ΔPE/EGFP*) (Anderson et al. 2000; Scholer et al. 1990; Yeom et al. 1996) into the 129.MOLF-Chr19 strain (see Methods). This transgene allows us to visualize GFP-labeled germ cells. The derived mouse strain is referred to as 129.MOLF-Chr19;*Oct4*-GFP. The *GOF-1/ΔPE/EGFP* transgene carries a deletion of the proximal enhancer element (ΔPE) of *Oct4* so that GFP is specifically expressed in germ cells but not in embryonal carcinoma (EC) cells (Yeom et al. 1996). GFP from the *Oct4*-GFP transgene can be detected in germ cells from embryonic day (E) 7.5-E8 (Anderson et al. 2000) until postnatal (PN) day 1.

We examined the testes of newborn mice (PN1) of the 129.MOLF-Chr19;*Oct4*-GFP strain by confocal microscopy. GFP-expressing germ cells were observed in the seminiferous tubules of the PN1 testes (Fig. 1E, F). Seven of the 11 PN1 testes examined from 129.MOLF-Chr19;*Oct4*-GFP appeared normal by light microscopy and confocal microscopy of GFP-expressing germ cells (Fig. 1B, E). However, four PN1 testes of the 129.MOLF-Chr19;*Oct4*-GFP strain showed reduction in GFP-expressing germ cells at specific locations (Fig. 1F). Histologic sections from these testes indicated blood-filled regions and proliferative clusters of transformed EC cells, which coexisted near seminiferous tubules containing germ cells (Fig. 1I). For a control for normal PN1 testes (or mouse line with low TGCT incidence), we examined PN1 testes of 129;*Oct4*-GFP mice where GFP-expressing germ cells were observed in the tubules (Fig. 1A, D, G).

Our results indicate that in the 129.MOLF-Chr19 strain, testes of newborn mice contain both GFP-expressing germ cells and transformed EC cells. GFP expression from *GOF-1/ΔPE/EGFP* is a reliable indication of retention of the germ cell state (Kehler et al. 2004) because *GOF-1/ΔPE/EGFP* expression is downregulated when cells exit the germ line lineage (Pesce et al. 1998; Yeom et al. 1996) to form EC cells. Our results indicate that not all germ cells in the genetically inbred 129.MOLF-Chr19 strain testes undergo transformation or transform at the same time, and there is a possibility that transformation may still be ongoing at the PN1 stage. Based on these confocal microscopy observations, we chose to include PN1 testes for differential gene expression analysis as described below.

A TGCT susceptibility locus in mid-Chr 19

The testicular tumor incidence of the males of the 129.MOLF-Chr19 strain ranges from 70% to 80% (Matin et al. 1999; Youngren et al. 2003). As a prelude to gene identification, we sought to map one of the TGCT susceptibility loci from the 129.MOLF-Chr19 strain. Previous mapping data (Youngren et al. 2003) had predicted five broad regions (regions I-V) that harbor TGCT susceptibility loci on mouse Chr 19. One 8.7 cM interval (region III) in mid-Chr 19 was predicted to contribute to a TGCT incidence of 30% in the 129.MOLF-Chr19 strain. To test if this region indeed contributes to TGCT incidence, we created a new congenic mouse strain (see Methods), congenic L1 (Fig. 2). Congenic L1 is homozygous for a 7.6-Mb region of MOLF-derived chromosome (between the SSLP markers D19Mit97 and D19Mit57) on the 129 strain background. Markers *D19Mit117* and *D19Mit135* are homozygous for 129 alleles.

We examined the testicular tumor incidence in adult males of congenic L1 and compared the incidence to the predicted 30% value. Twenty-two of the 76 males (29%; $p = 0.96$) had testicular tumors. Thus, tumor incidence of congenic L1 strain confirms the predicted 30% value and maps a 7.6 Mb region in mid-Chr 19 (locus 1) that independently contributes to a TGCT incidence of 30%. Thus, locus 1 maps one of the five tumor susceptibility loci from the 129.MOLF-Chr19 strain.

Locus 1 contains approximately 60 genes (MGI, http://www.informatics.jax.org/) (Supplementary Table 1) Most of this region is orthologous to human Chr9p24.1–24.3. In humans, chromosomal region 9p24.3 has been implicated in the failure of testicular development, feminization, gonadal dysgenesis, and sex reversal in XY patients (McDonald et al. 1997; Muroya et al. 2000; Raymond et al. 1999; Shan et al. 2000; Veitia et al. 1997). The genes *Dmrt1*, *Dmrt2*, and *Dmrt3* map to 9p24.3 and to locus 1. In humans, *Dmrt1* is involved in testis differentiation (Smith et al. 1999) and has a gonad-specific and sexually dimorphic expression profile during embryogenesis in vertebrates. It is also involved in regulation of sex-associated expression patterns in *Drosophila* and *C. elegans* (Burtis and Baker 1989; Raymond et al. 1998; Shen and Hodgkin 1988).

Candidate TGCT susceptibility genes from locus 1 would include genes with single nucleotide polymorphisms (SNPs) in the coding regions (especially nonsynonymous SNPs, nsSNPs), regulatory regions, or splice sites. These SNPs would be expected to alter coding sequences to affect the structure and function of the gene-encoded proteins or alter expression levels of the gene. First, we examined nsSNP differences between 129 and MOLF strains for Chr 19 locus 1 genes in the database (MGI, http://www.informatics.jax.org/javawi2/servlet/WI-Fetch?page=snpQF). However, the data are sparse. Therefore, we sequenced the cDNA of eight genes from the 129 and MOLF strains that map within locus 1 (Supplementary Fig. 1). Six genes had at least one non-synonymous change within their coding regions in the 129.MOLF-Chr19 (MOLF chromosome) (Supplementary Fig. 1, Supplementary Table 1). Thus, nsSNPs are frequent between coding sequences of the MOLF and 129 chromosomes. This is not surprising because the MOLF strain, although a fertile, inbred strain, is of the subspecies *M. m. molossinus*, which is evolutionarily distant from the 129 strain (*M. m. musculus*) (Silver 1995). The strain was initially chosen for linkage crosses because of the high rate of polymorphic SSLP sequences between MOLF and 129, and these two strains were successfully used to establish linkage for TGCT susceptibility loci on Chr 19 (Collin et al. 1996; Matin et al. 1999). However, this makes it more difficult to pinpoint TGCT susceptibility genes from 129.MOLF-Chr19 because SNPs are relatively frequent in neighboring genes. One way to pinpoint susceptibility genes in 129.MOLF-Chr19 would be to create congenic strains containing smaller regions (1 Mb or less) of the MOLF-derived chromosome such that only a few genes are present within the segment and need to be evaluated as candidate TGCT susceptibility genes.

Gene expression differences between the 129 and the 129.MOLF-Chr19 strain

As an alternate approach to narrow the candidate TGCT susceptibility genes from the 60 genes in locus 1, we compared gene expression profiles of the early gonads from the 129.MOLF-Chr19 and 129 strains using microarrays (GeneChip® Mouse Genome 430 2.0; Affymetrix, Santa Clara, CA).

For gene expression profiling, we used male gonads from different developmental stages, i.e., E13.5 and PN1, from the 129.MOLF-Chr19 and the 129 strains. The idea was to detect the common gene expression changes in the gonads at stages when germ cells are known to transform to EC cells. The E13.5 stage was chosen because tumor development is reported to start around E13.5 in 129 strains (Stevens 1973b; Stevens and Hummel 1957). PN1 stage gonads were chosen because our confocal microscopy studies (described above) of PN1 testes

of the 129.MOLF-Chr19 strain showed that both germ cells and EC cells are present at this stage, suggesting that germ cell transformation may be ongoing at this stage.

We also compared gene expression differences in gonads with that of embryos to determine whether gene expression differences are specific to the gonads. Our goal was to identify gene (s) whose expression is consistently changed in the gonads at the two stages, E13.5 and PN1, in the 129.MOLF-Chr19 strain because these would likely be candidate TGCT susceptibility gene(s).

Figure 3A shows the three different tissue samples collected from the 129.MOLF-Chr19 and the 129 strains: gonads (genital ridges) dissected from male E13.5 embryos and from PN1 mice and male embryos at E13.5. Because tumor incidence in 129.MOLF-Chr19 is approximately 80%, we anticipated that gene expression changes could be masked because approximately 20% of cells/tissues within a sample may have normal levels of gene expression or 20% of the testes may have normal gene expression. For a similar reason, we chose not to use the congenic L1 strain because we anticipated that in this strain gene expression changes would be even more severely masked because approximately 70% of cells/tissues within congenic L1 samples may have normal levels of gene expression. Thus, to minimize the effect of individual samples and to isolate sufficient RNA for microarray analysis from these small-size gonads, we pooled RNA from multiple samples from the 129 and 129.MOLF-Chr19 strains (Supplementary Table 2).

Six RNA-pooled samples were prepared (Fig. 3A, Supplementary Table 2): E13.5 gonad (genital ridge) RNA from males of 129 (129-GR) and 129.MOLF-Chr19 (CSS-GR); PN1 testes RNA from 129 (129-NBT) and 129.MOLF-Chr19 (CSS-NBT); and E13.5 embryo RNA from males of 129 (129-E) and 129.MOLF-Chr19 (CSS-E). The six RNA samples were hybridized to six Affymetrix mouse genome GeneChips individually (see Methods). Hierarchical clustering analysis revealed a dendrogram in which gene expression profiles of the same tissue type clustered together (Fig. 3B). Profiles of the gonads E13.5 and PN1 were related more closely than to those of embryos.

Comparison of the expression profiles of E13.5 gonads from 129.MOLF-Chr19 and 129 revealed ten genes with more than a twofold difference in expression levels (Fig. 3A, Supplementary Table 3A). Six of the ten genes mapped to Chr 19. For the PN1 testes, 266 genes showed significant fold changes between the two strains and of these 13 genes mapped to Chr 19 (Fig. 3A, Supplementary Table 3C).

For the E13.5 embryos, 35 genes showed a greater than twofold change in expression between the 129.MOLF-Chr19 and 129 strains and 5 of 35 genes mapped to Chr 19 (Fig. 3A, Supplementary Table 3B).

By analyzing the data of differentially expressed genes present in the three samples, as well as selecting those that map to Chr 19, we were able to exclude a majority of the genes but found three genes in common. The three genes, *Zfp162*, *D19Bwg1357e*, and *Cox15*, mapped to Chr 19 and were found to be downregulated in the 129.MOLF-Chr19 strain E13.5 and PN1 gonads as well as E13.5 embryos. These genes have not been previously implicated in testicular tumorigenesis and are novel TGCT candidate susceptibility genes. *D19Bwg1357e* maps to locus 1 and is therefore a candidate TGCT susceptibility gene from locus 1.

Our analysis focused on identifying genes whose expression is consistently changed in the gonads of the 129.MOLF-Chr19 strain at two different stages, E13.5 and PN1. By using this criterion, we may likely be excluding other TGCT susceptibility genes whose expression is unchanged or changed at either E13.5 or PN1 but not at both stages. Despite this, we have been

able to identify three candidate genes that show robust and consistent changes. Moreover, this approach has allowed us to pinpoint one gene from a list of 60 genes present in locus 1.

Validation of gene expression differences by qRT-PCR

To validate the gene expression changes of the three Chr 19 genes (*D19Bwg1357e*, *Zfp162*, and *Cox15*) from the microarray data, quantitative real-time polymerase chain reaction (qRT-PCR) was performed. The expression changes were validated using the same RNA pool (E13.5 gonads, PN1 testes, and E13.5 embryo pool) used for the microarray and a new independent pool of RNA from PN1 testes (pool of 60 testes) (Table 2). Although the *Dmrt* genes map within locus 1, gene expression differences for the *Dmrt* genes were not observed between the 129.MOLF-Chr19 and 129 gonads in either microarray analysis or by qRT-PCR (data not shown). Thus, the *Dmrt* genes may not be TGCT candidate genes for the 129.MOLF-Chr19 strain.

The gene *D19Bwg1357e* maps within locus 1. *Zfp162* maps to proximal Chr 19 (TGCT susceptibility locus, region I) and *Cox15* maps distal to locus 1 (TGCT susceptibility locus, region V) (Youngren et al. 2003) (Fig. 3A). qRT-PCR indicated that *D19Bwg1357e* expression is downregulated approximately twofold in the gonads and embryos of 129.MOLF-Chr19.

Because the expression of the three genes is downregulated in 129.MOLF-Chr19 compared with 129, it is likely that these genes are functioning as hypomorphs in the 129.MOLF-Chr19 strain. Thus, complete loss of these genes on the 129 background would be predicted to cause an even higher testicular tumor incidence. To test this, future work will examine the TGCT incidence in mice with targeted deletion of these genes.

Comparative expression of microRNAs from Chr 19 of 129 and 129.MOLF-Chr19 strains

MicroRNAs are a class of small RNAs that fine-tune gene expression of an extensive number of other (target) mRNAs during development, differentiation, and cancer development. Gene regulation by microRNAs has been demonstrated in testicular cancer. Two microRNAs, human miR-372 and miR-373, were found to be expressed in human TGCT cell lines and primary seminomas (Voorhoeve et al. 2006). These two microRNA act as oncogenes that collaborate with RAS in cellular transformation (Voorhoeve et al. 2006). To determine if microRNAs are important TGCT factors for germ cell tumor development in the 129.MOLF-Chr19 strain, we examined the expression of known and predicted microRNAs that map to mouse Chr 19 and compared the expression levels in 129 and 129.MOLF-Chr19 gonads and testicular tumors using RNase protection assays (RPAs). Six predicted microRNAs map to mouse Chr 19 (miRBase of Sanger: http:// www.microrna.sanger.ac.uk/). They are mmu-miR-101b, mmu-miR-107, mmu-miR-146b, mmu-miR-192, mmumiR-194-2, and mmu-miR-204. We also examined the expression of mmu-miR-290, mmu-miR-294, and mmumiR-295, which are the predicted mouse orthologs of human miR-372 and 373. The map locations of these three miRNAs on mouse chromosomes are not known.

Small RNA samples (sRNAs, RNAs < 200 nt long) were isolated from adult testes (PN40), PN1 testes, and E13.5 embryos from 129 and 129.MOLF-Chr19 strains and from 129.MOLF-Chr19 testicular tumors. Detection of microRNA expression in the sRNA samples from the various tissues was performed by RNase protection analysis (RPA) using radiolabeled antisense RNA probes.

RPA detected expression of only mmu-miR-107 in the sRNA samples derived from testes, testicular tumors, and embryos of 129 (Supplementary Fig. 2). Ubiquitously expressed miR-16, which maps to Chrs 3 and 14, was used as experimental control. We compared the expression levels of mmu-miR-107 in embryos, gonads, and tumors of 129.MOLF-Chr19 to those of 129.

For an accurate estimation, we first determined the sRNA input amount best suited for comparison of expression level differences between samples (Fig. 4A, B). We determined that use of 0.1 μg sRNA would allow the assay to be in the linear range and be able to detect a twofold change. An internal control of radiolabeled U6 sRNA probe was used.

Our results show that miR-107 levels in the PN1 testes and adult testes of the 129.MOLF-Chr19 were consistently lower compared with those in the 129 strain (Fig. 4C, D). The significance of slightly lower expression of miR-107 in gonadal tissues of 129.MOLF-Chr19 is not clear at present. In contrast, miR-107 was increased twofold in testicular tumors from the 129.MOLF-Chr19 strain. There was no significant difference in expression levels of miR-107 in the embryos of 129 and 129.MOLF-Chr19.

To identify possible candidate genes whose expression may be upregulated in PN1 testes of 129.MOLF-Chr19 due to decreased miR-107, we examined the 266 genes that are differentially expressed between the 129 and 129.MOLF-Chr19 PN1 testes. Two genes, which are predicted targets of miR-107 (http://www.microrna.sanger.ac.uk/), tropomodulin 1 (*Tmod1*) and *Wipi1*, were upregulated approximately three- and twofold, respectively, in 129.MOLF-Chr19 PN1 gonads (Supplementary Table 3C). The role of *Tmod1* and *Wipi1* in TGCT development will be examined further in the future.

Discussion

We examined the etiology of testicular germ cell tumor development in the 129.MOLF-Chr 19 strain. Expression of GFP from the *GOF-1/ΔPE/EGFP* transgene in the PN1 testes indicates retention of normal germ cells in the midst of transformed cells. Thus, transformation of the germ cells appears to be at a gradual pace in the 129.MOLF-Chr19 strain. It is likely that a certain proportion of the germ cells becomes transformed in the midst of normal germ cells. The intriguing question is why some germ cells transform to EC cells, whereas others apparently remain normal and contribute to fertility of the 129.MOLF-Chr19 strain.

To identify the cause of germ cell transformation and identify candidate TGCT susceptibility genes from the 129.MOLF-Chr19 strain, we used different approaches. First, we made a new congenic strain harboring a 7.6Mb region of MOLF-derived chromosome (locus 1). This strain has approximately 30% TGCT incidence implicating the presence of TGCT candidate gene(s) within locus 1. Locus 1 is one of the five TGCT susceptibility loci from 129.MOLF-Chr19.

To pinpoint candidate TGCT genes, we examined gene expression differences for genes on Chr 19 from the 129.MOLF-Chr19 and 129 strains. Gene expression differences can be the result of polymorphisms or SNPs in the regulatory regions of genes, which result in lower mRNA levels from one strain. Alternatively, the stability of the mRNA may be affected by SNPs or sequence changes at the 3′-untranslated region (Ross 1995).

To compare gene expression profiles between the 129.MOLF-Chr19 and 129 strains, we chose to examine the gonads from the two strains at stages when the transformation process of germ cells to EC cells is taking place. Stevens' (1966,1970) transplantation experiments indicated that transformation occurred in the gonads (genital ridges) at stages between E11.5 and E13.5 in the 129 strain. We therefore chose to examine the expression profiles of E13.5 gonads. Our confocal microscopy data indicated that germ cells of PN1 testes from 129.MOLF-Chr19 may also be undergoing transformation at this stage. Therefore, we also compared gene expression in PN1 testes. Comparison of the expression data from the two gonadal sources at different stages allowed us to exclude the majority of the genes and identify three genes in common. The expression levels of these three genes were consistently lower in the gonads at the two developmental stages. Their expression levels were also lower in the E13.5 embryo.

There are a number of limitations in the approaches used here to identify TGCT susceptibility genes. First, in cases where probe sets in microarrays and primers used for qRT-PCR overlap, as is the case for the *Zfp162* gene, SNPs may interfere with hybridizations in both techniques and produce false-positive results. Second, one limitation of our microarray studies is that we cannot estimate how many other real differences are present and we may have excluded a number of other candidate TGCT susceptibility genes. Moreover, it is possible that genes that are differentially regulated between 129 and 129.MOLF-Chr19 may not be the cause of tumor development, but the expression differences are the result of the physical location of the genes on the MOLF chromosome. Keeping these caveats in mind, this approach nonetheless has allowed us to identify and focus our attention on a limited number (3) of TGCT susceptibility candidate genes. The decreased expression of the three genes from microarray analysis was verified by qRT-PCR.

One of the genes, *D19Bwg1357e*, mapped within locus 1. The other two genes, *Zfp162* and *Cox15*, also mapped to Chr 19 but were outside of locus 1. *Zfp162* maps to one of the predicted TGCT susceptibility loci, region I (a 12cM interval) (Youngren et al. 2003). *Cox15* maps to the boundary of region V (a 30.8cM interval) (Youngren et al. 2003). Unlike locus 1, the boundaries of the other predicted regions, including regions I and V, have not been narrowed further. All three genes were downregulated in whole embryos and in gonads from E13.5 and PN1 stages. Thus, although the expressions of *D19Bwg1357e*, *Zfp162*, and *Cox15* may not be restricted to the gonads, the negative consequence of lower expression predominantly affects the gonads to result in germ cell tumor development. One possibility is that germ cells are especially sensitive to the lower expression levels of the genes and their function is critical in germ cells.

D19Bwg1357e and *Zfp162* are novel genes with unknown function. The *D19Bwg1357e* gene is one of four genes in the mouse with pumilio or Puf RNA-binding domains. Other members of this family in mice include Pumilio-1 and Pumilio-2 genes, the orthologs of which are expressed in human embryonic and germline stem cells (Moore et al. 2003). Expression of *D19Bwg1357e* has been detected in purified PGCs isolated from embryos at E10.5 and E12.5 stages (Molyneaux et al. 2004). Sequence analysis of the *D19Bwg1357e* gene from the 129.MOLF-Chr19 strain indicated the presence of multiple SNPs in the coding region of *D19Bwg1357e* (Supplementary Fig. 1). One SNP (M514I; methionine changed to isoleucine at the 514th amino acid) causes a nonsynonymous change in the *D19Bwg1357e*-encoded protein from the 129.MOLF-Chr19 strain.

Zfp162 is another RNA-binding protein with zinc knuckle motif (Wrehlke et al. 1999). It may act as a splicing factor. *Cox15* is a homolog of yeast COX15, cytochrome c oxidase assembly protein, and in humans COX15 is a mitochondrial protein involved in the synthesis of heme A (Antonicka et al. 2003 ; Glerum et al. 1997).

To identify candidate microRNAs from Chr 19 that influence TGCT susceptibility, we examined the expression of known Chr 19 microRNAs and found that mmumiR-107 was increased twofold in testicular tumors from the 129.MOLF-Chr19 strain. One interpretation is that germ cells express lower levels of mmu-miR-107 compared to the differentiated cell types that are observed in testicular tumors (Fig. 1K) and the increase in levels may reflect the role of mmu-miR-107 in differentiated cell types. Another possibility is that increased miR-107 levels are oncogenic. This is supported by the report that expression of the human ortholog of miR-107 is a distinctive feature associated with pancreatic tumorigenesis (Roldo et al. 2006). Available programs such as Target-Scan (http://www.targetscan.org/) indicate a number of putative gene targets for miR-107. Two candidate target genes of miR-107, *Tmod1* and *Wipi1*, were found to be upregulated in the 129.MOLF-Chr19 PN1 testes. The role of these

predicted target genes in germ cells and tumors will have to be experimentally ascertained in future experiments.

In summary, we have found four candidate novel TGCT susceptibility genes from the chromosome substitution strain, 129.MOLF-Chr19. A number of questions remain to be answered regarding TGCT susceptibility genes from the 129.MOLF-Chr19 strain. Do the TGCT susceptibility genes function individually or is lowered expression of a combination of genes necessary for tumor development in 129.MOLF-Chr19? Also, because more than one gene is responsible for TGCT development in 129.MOLF-Chr19 mice, this raises the question whether tumor development in individual 129.MOLF-Chr19 mice occurs through the same pathway. The identification of candidate TGCT susceptibility genes, as described here, is the first step toward a systematic examination of the role of individual genes in TGCT development. Our results demonstrate that the 129.MOLF-Chr 19 strain serves as a model strain to elucidate the complex genetics and biology of PGC transformation and TGCT development. Genes identified in the 129.MOLF-Chr 19 strain may in the future serve as useful disease markers for TGCTs in humans.

Supplementary Material

Refer to Web version on PubMed Central for supplementary material.

Acknowledgments

The authors thank Henry Adams and micro-array core facility personnel at the M.D. Anderson Cancer Center (Cancer Center Support Grant CA #16672) for invaluable technical support. This work was supported by National Cancer Institute grant CA093754 and David Carmine Cancer Research Fund to AM.

Abbreviations

SNP, single nucleotide polymorphism; nt, nucleotide; qRT-PCR, quantitative real-time polymerase chain reaction; Chr, chromosome; TGCT, testicular germ cell tumor; PN1, postnatal day 1; E, embryonic day.

References

Anderson R, Copeland TK, Scholer H, Heasman J, Wylie C. The onset of germ cell migration in the mouse embryo. Mech Dev 2000;91:61–68. [PubMed: 10704831]

Antonicka H, Mattman A, Carlson CG, Glerum DM, Hoffbuhr KC, et al. Mutations in COX15 produce a defect in the mitochondrial heme biosynthetic pathway, causing early-onset fatal hypertrophic cardiomyopathy. Am J Hum Genet 2003;72:101–114. [PubMed: 12474143]

Burtis KC, Baker BS. Drosophila doublesex gene controls somatic sexual differentiation by producing alternatively spliced mRNAs encoding related sex-specific polypeptides. Cell 1989;56:997–1010. [PubMed: 2493994]

Collin GB, Asada Y, Varnum DS, Nadeau JH. DNA pooling as a quick method for finding candidate linkages in multigenic trait analysis: an example involving susceptibility to germ cell tumors. Mamm Genome 1996;7:68–70. [PubMed: 8903734]

Crockford GP, Linger R, Hockley S, Dudakia D, Johnson L, et al. Genome-wide linkage screen for testicular germ cell tumour susceptibility loci. Hum Mol Genet 2006;15:443–451. [PubMed: 16407372]

Dieckmann K-P, Skakkebaek NE. Carcinoma in situ of the testis: review of biological and clinical features. Int J Cancer 1999;83:815–822. [PubMed: 10597201]

Forman D, Oliver RT, Brett AR, Marsh SG, Moses JH, et al. Familial testicular cancer: a report of the UK family register, estimation of risk and an HLA class 1 sib-pair analysis. Br J Cancer 1992;65:255–262. [PubMed: 1739626]

Glerum DM, Muroff I, Jin C, Tzagoloff A. COX15 codes for a mitochondrial protein essential for the assembly of yeast cytochrome oxidase. J Biol Chem 1997;272:19088–19094. [PubMed: 9228094]

Harland SJ, Cook PA, Fossa SD, Horwich A, Mead GM, et al. Intratubular germ cell neoplasia of the contralateral testis in testicular cancer: defining a high risk group. J Urol 1998;160:1353–1357. [PubMed: 9751353]

Heimdal K, Olsson H, Tretli S, Flodgren P, Borresen AL, et al. Familial testicular cancer in Norway and southern Sweden. Br J Cancer 1996;73:964–969. [PubMed: 8611416]

Hemminki K, Li X. Familial risk in testicular cancer as a clue to a heritable and environmental aetiology. Br J Cancer 2004;90:1765–1770. [PubMed: 15208620]

Horwich A, Shipley J, Huddart R. Testicular germ-cell cancer. Lancet 2006;367:754–765. [PubMed: 16517276]

Ilson DH, Bosl GJ, Motzer R, Dmitrovsky E, Chaganti RSK. Genetic analysis of germ cell tumors: current progress and future prospects. Hematol Oncol Clin North Am 1991;5:1271–1283. [PubMed: 1663944]

Jacobsen R, Bostofte E, Engholm G, Hansen J, Olsen JH, et al. Risk of testicular cancer in men with abnormal semen characteristics: cohort study. BMJ 2000;321:789–792. [PubMed: 11009515]

Ju Z, Kapoor M, Newton K, Cheon K, Ramaswamy A, et al. Global detection of molecular changes reveals concurrent alteration of several biological pathways in nonsmall cell lung cancer cells. Mol Genet Genomics 2005;274:141–154. [PubMed: 16049682]

Kawakami T, Zhang C, Okada Y, Okamoto K. Erasure of methylation imprint at the promoter and CTCF-binding site upstream of H19 in human testicular germ cell tumors of adolescents indicate their fetal germ cell origin. Oncogene 2006;25:3225–3236. [PubMed: 16434968]

Kehler J, Tolkunova E, Koschorz B, Pesce M, Gentile L, et al. Oct4 is required for primordial germ cell survival. EMBO J 2004;5:1078–1083.

Li C, Wong W-H. Model-based analysis of oligonucleotide arrays: expression index computation and outlier detection. Proc Natl Acad Sci U S A 2001;98:31–36. [PubMed: 11134512]

Looijenga LHJ, Stoop H, de Leeuw HP, de Gouveia Brazao CA, Gillis AJ, et al. POU5F1 (OCT3/4) identifies cells with pluripotent potential in human germ cell tumors. Cancer Res 2003;63:2244–2250. [PubMed: 12727846]

Matin A, Collin GB, Asada Y, Varnum D, Nadeau JH. Susceptibility to testicular germ-cell tumours in a 129.MOLF-Chr 19 chromosome substitution strain. Nat Genet 1999;23:237–240. [PubMed: 10508525]

McDonald MT, Flejter W, Sheldon S, Putzi MJ, Gorski JL. XY sex reversal and gonadal dysgenesis due to 9p24 monosomy. Am J Med Genet 1997;73:321–326. [PubMed: 9415692]

Molyneaux KA, Wang YC, Schaible K, Wylie C. Transcriptional profiling identifies genes differentially expressed during and after migration in murine primordial germ cells. Gene Exp Patterns 2004;4:167–181.

Moore FL, Jaruzelska J, Fox MS, Urano J, Firpo MT, et al. Human pumilio-2 is expressed in embryonic stem cells and germ cells and interacts with DAZ (Deleted in AZoospermia) and DAZ-like proteins. Proc Natl Acad Sci U S A 2003;100:538–543. [PubMed: 12511597]

Muroya K, Okuyama T, Goishi K, Ogiso Y, Fukuda S, et al. Sex-determining gene(s) on distal 9p: clinical and molecular studies in six cases. J Clin Endocr Metab 2000;85:3094–3100. [PubMed: 10999792]

Oosterhuis JW, Looijenga LHJ. Testicular germ-cell tumours in a broader perspective. Nat Rev Cancer 2005;5:210–222. [PubMed: 15738984]

Pesce M, Gross MK, Scholer HR. In line with our ancestors: Oct-4 and the mammalian germ. Bioessays 1998;20:722–732. [PubMed: 9819561]

Rapley EA, Crockford GP, Teare D, Biggs P, Seal S, et al. Localization to Xq27 of a susceptibility gene for testicular germ-cell tumors. Nat Genet 2000;24:197–200. [PubMed: 10655070]

Raymond CS, Shamu CE, Shen MM, Seifert KJ, Hirsch B, et al. Evidence for evolutionary conservation of sex-determining genes. Nature 1998;391:691–695. [PubMed: 9490411]

Raymond CS, Parker ED, Kettlewell JR, Brown LG, Page DC, et al. A region of human chromosome 9p required for testis development contains two genes related to known sexual regulators. Hum Mol Genet 1999;8:989–996. [PubMed: 10332030]

Rescorla FJ. Pediatric germ cell tumors. Semin Surg Oncol 1999;16:144–158. [PubMed: 9988869]

Roldo C, Missiaglia E, Hagan JP, Falconi M, Capelli P, et al. MicroRNA expression abnormalities in pancreatic endocrine and acinar tumors are associated with distinctive pathological features and clinical behaviour. J Clin Oncol 2006;24:4677–4684. [PubMed: 16966691]

Ross J. mRNA stability in mammalian cells. Microbiol Rev 1995;59:423–450. [PubMed: 7565413]

Scholer HR, Dressler GR, Balling R, Rohdewohld H, Gruss P. Oct-4: a germline-specific transcription factor mapping to the mouse t-complex. EMBO J 1990;9:2185–2195. [PubMed: 2357966]

Shan Z, Zabel B, Trautmann U, Hillig U, Ottolenghi C, et al. FISH mapping of the sex-reversal region on human chromosome 9p in two XY females and in primates. Eur J Hum Genet 2000;8:167–173. [PubMed: 10780781]

Shen MM, Hodgkin J. Mab-3, a gene required for sex-specific yolk protein expression and a male-specific lineage in *C. elegans*. Cell 1988;54:1019–1031. [PubMed: 3046751]

Silver, LM. Mouse genetics: concepts and applications. Oxford University Press; New York: 1995.

Skakkebaek NE, Berthelsen JG, Giwercman A, Muller J. Carcinoma-in-situ of the testis: possible origin from gonocytes and precursor of all types of germ cell tumours except spermatocytoma. Int J Androl 1987;10:19–28. [PubMed: 3034791]

Skakkebaek NE, Holm M, Hoei-Hansen C, Jorgensen N, Rajpert-De Meyts E. Association between testicular dysgenesis syndrome (TDS) and testicular neoplasia: evidence from 20 adult patients with signs of maldevelopment of the testis. APMIS 2003;111:1–11. [PubMed: 12752226]

Smiraglia DJ, Szymanska J, Kraggerud SM, Lothe RA, Peltomaki P, et al. Distinct epigenetic phenotypes in seminomatous and nonseminomatous testicular germ cell tumors. Oncogene 2002;21:3909–3916. [PubMed: 12032829]

Smith CA, McClive PJ, Western PS, Reed KJ, Sinclair AH. Conservation of a sex-determining gene. Nature 1999;402:601–602. [PubMed: 10604464]

Stevens LC. Development of resistance to teratocarcinogeneis by primordial germ cells in mice. J Natl Cancer Inst 1966;37:859–867. [PubMed: 6005945]

Stevens LC. Origin of testicular teratomas from primordial germ cells in mice. J Natl Cancer Inst 1967;38:549–552. [PubMed: 6025005]

Stevens LC. Experimental production of testicular teratomas in mice of strains 129, A/He, and their F1 hybrids. J Natl Cancer Inst 1970;44:923–929. [PubMed: 11515059]

Stevens LC. A developmental genetic approach to the study of teratocarcinogenesis. BioScience 1973a; 23:169–172.

Stevens LC. A new inbred subline of mice (129/terSv) with a high incidence of spontaneous congenital testicular teratomas. J Natl Cancer Inst 1973b;50:235–242. [PubMed: 4692863]

Stevens LC, Hummel KP. A description of spontaneous congenital testicular teratomas in strain 129 mice. J Natl Cancer Inst 1957;18:719–747. [PubMed: 13502692]

Tollerud DJ, Blattner WA, Fraser MC, Brown LM, Pottern L, et al. Familial testicular cancer and urogenital developmental anomalies. Cancer 1985;55:1849–1854. [PubMed: 2858262]

Veitia R, Nunes M, Brauner R, Doco-Fenzy M, Joanny-Flinois O, et al. Deletions of distal 9p associated with 46,XY male to female sex reversal: definition of the breakpoints at 9p23.3-p24.1. Genomics 1997;41:271–274. [PubMed: 9143505]

Voorhoeve PM, le Sage C, Schrier M, Gillis AJM, Stoop H, et al. A genetic screen implicates miRNA-372 and miRNA-373 as oncogenes in testicular germ cell tumors. Cell 2006;124:1169–1181. [PubMed: 16564011]

Wrehlke C, Wiedemeyer WR, Schmitt-Wrede HP, Mincheva A, Lichter P, et al. Genomic organization of mouse gene *zfp162*. DNA Cell Biol 1999;18:419–428. [PubMed: 10360842]

Yeom YI, Fuhrmann G, Ovitt CE, Brehm A, Ohbo K, et al. Germline regulatory element of Oct-4 specific for the totipotent cycle of embryonal cells. Development 1996;122:881–894. [PubMed: 8631266]

Youngren KK, Nadeau JH, Matin A. Testicular cancer susceptibility in the 129.MOLF-Chr 19 mouse strain: additive effects, gene interactions and epigenetic modifications. Hum Mol Genet 2003;12:389–398. [PubMed: 12566386]

Youngren KK, Coveney D, Peng X, Bhattacharya C, Schmidt LS, et al. The Ter mutation in the dead end gene causes germ cell loss and testicular germ cell tumours. Nature 2005;435:360–364. [PubMed: 15902260]

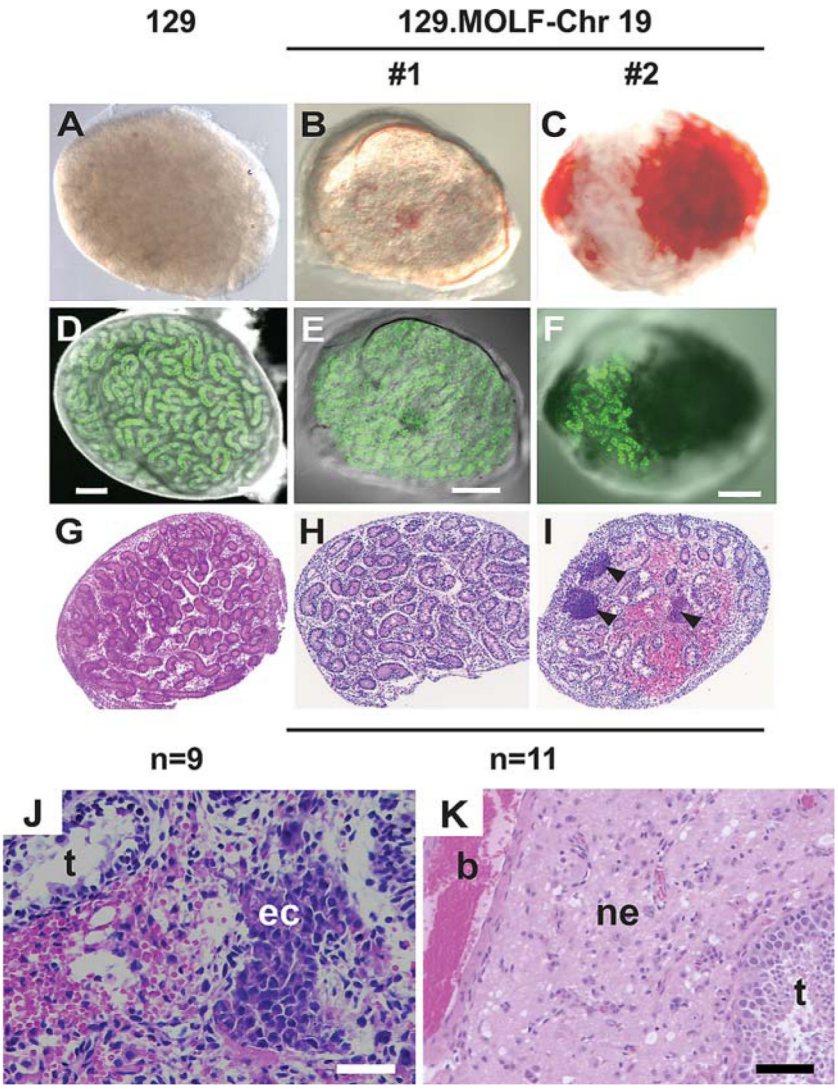

Fig. 1.

Morphologic comparison of PN1 testes from the 129 and 129.MOLF-Chr19 strains. A-C PN1 testes observed using reflected light under the stereomicroscope from the (A) 129 and (B, C) 129.MOLF-Chr19 strains. The same testis was observed for GFP fluorescence by confocal microscope to observe GFP-expressing germ cells within the seminiferous tubules of the (D) 129 and (E, F) 129.MOLF-Chr19 strains. GFP-expressing germ cells are found in the testes of the 129.MOLF-Chr19 strain (E, F). Scale bar = 200 μm. H&E-stained histologic cross sections of the PN1 testes from the (G) 129 and (H, I) 129.MOLF-Chr19 strains. Arrows indicate clusters of proliferating embryonal carcinoma (EC) cells. J Higher magnification showing EC cells (ec) from (I) adjacent to seminiferous tubules (t). Scale bar = 15 μm. K H&E-stained histologic cross section through adult (PN40) testicular germ cell tumor of the 129.MOLF-Chr19 strain. Neuroepithelial cells (ne) and blood (b) are present adjacent to seminiferous tubules (t). Scale bar = 30 μm

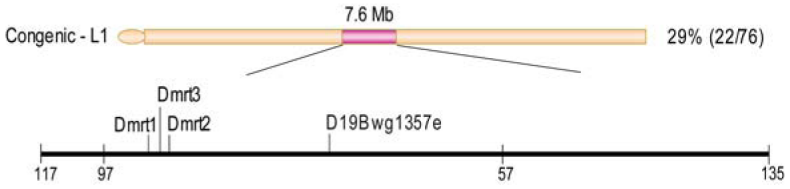

Fig. 2.

Boundaries of congenic-L1. Schematic diagram of mouse Chr 19. The areas in red represent regions that are homozygous for MOLF alleles, whereas areas in yellow represent regions homozygous for 129 alleles. SSLP markers *D19Mit97* and *D19Mit57* define the 7.6Mb region in congenic-L1 and are homozygous for MOLF alleles. The region is flanked by *D19Mit117* and *D19Mit135* which are homozygous for 129 alleles. Twenty-two of 76 (29%) male mice of congenic-L1 had testicular tumors. In contrast, 70%–80% of the 129.MOLF-Chr19 strain develop testicular tumors. Approximately 60 genes map to the congenic-L1 (locus 1) region

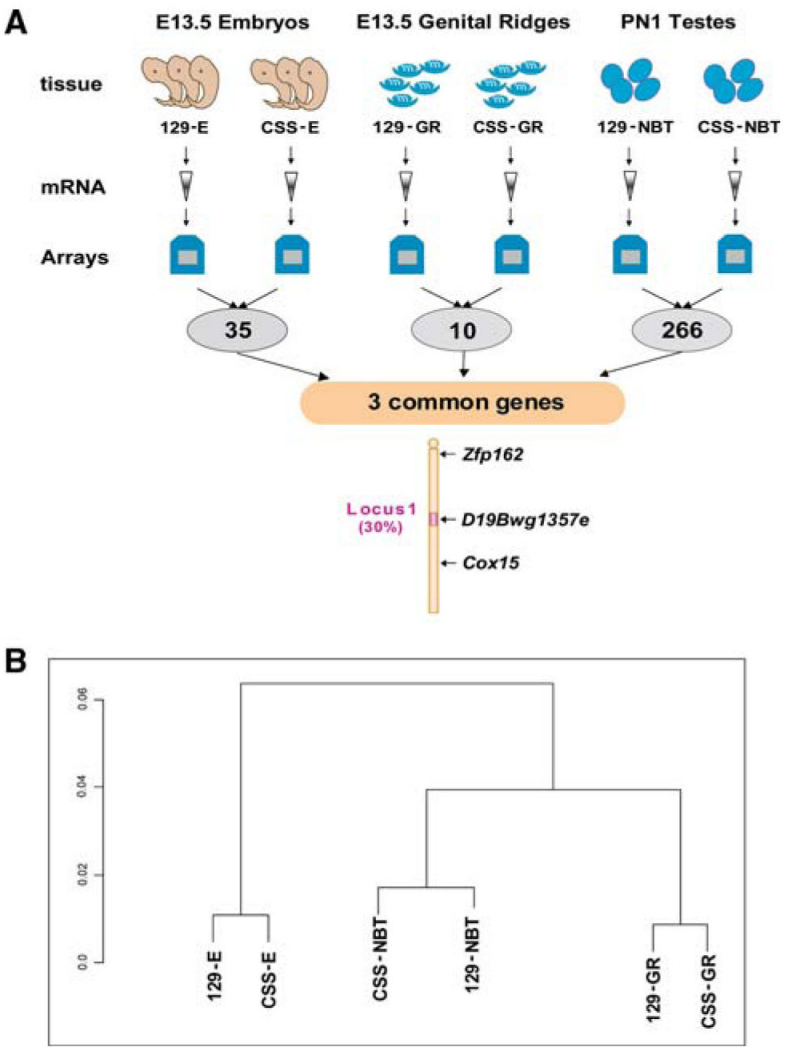

Fig. 3.

Gene expression differences between the 129 and 129.MOLF-Chr19 strains. A Male embryos at E13.5, genital ridges (gonads) dissected from E13.5 male embryos, and testes from newborn mice (PN1) were harvested from the 129 and 129.MOLF-Chr19 strains. Total RNA was extracted from the pooled tissues and applied to Affymetrix GeneChip® Mouse Genome 430 2.0. Analysis of gene expression indicated 35 genes with a greater than twofold difference in E13.5 embryos of 129.MOLF-Chr19 (CSS-E) compared to 129 (129-E) strains; 10 genes with a greater than twofold difference in the genital ridges of 129.MOLF-Chr19 (CSS-GR) compared to 129 (129-GR); and 266 genes with a greater than twofold difference in the PN1 testes of 129.MOLF-Chr19 (CSS-NBT) compared to 129 (129-NBT). When these three gene lists were compared, three genes (*Zfp162*, *D19Bwg1357e*, and *Cox15*) were found in common and these genes were also downregulated in the 129.MOLF-Chr19 tissues. All three genes map to mouse Chr 19 and *D19Bwg1357e* maps to locus 1, which is responsible for a 30% incidence of TGCTs. B Dendogram indicating clustering of gene expression profiles of the embryo samples (129-E and CSS-E), genital ridge samples (129-GR and CSS-GR), and PN1 testes samples (129-NBT and CSS-NBT)

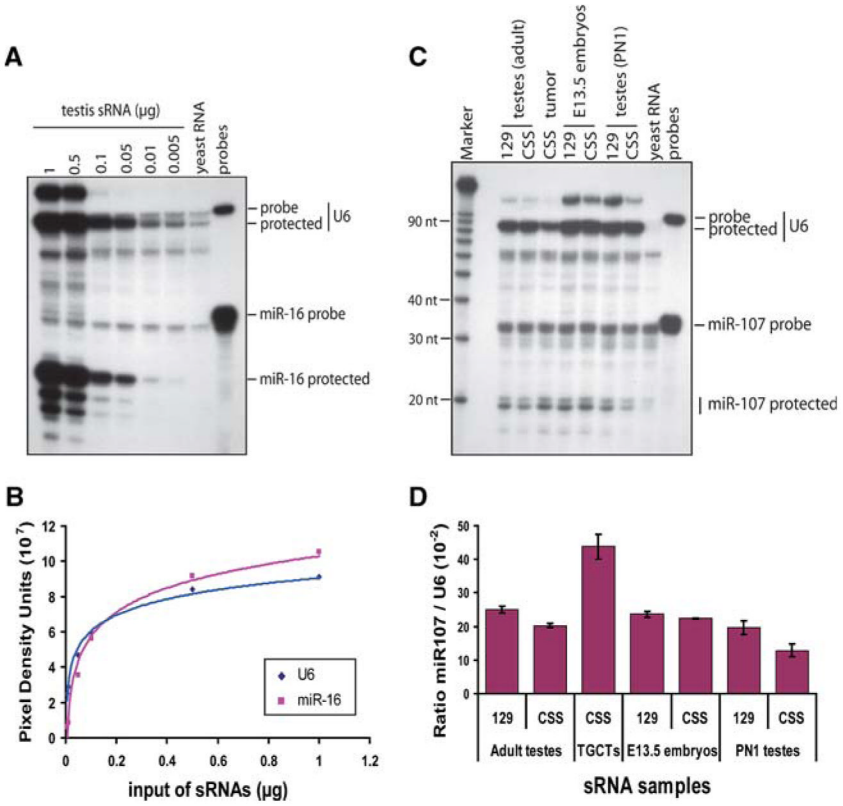

Fig. 4.

Expression of mmu-miR-107 in 129.MOLF-Chr19 and 129 tissues. A Determining the optimum concentration of small RNA (sRNA) for hybridization to ^{32}P-labeled RNA probe. sRNA (0.005-1 μg) from 129 testis was incubated in solution with maximum amount of ^{32}P-labeled control probes, mmu-miR-16 and U6. Upon hybridization, the RNA-RNA hybrid was protected from RNase A/RNase T digestion. The protected fragments were separated on 15% denaturing polyacrylamide gel before detection by autoradiography. Yeast RNA was used as control. B Plot of sRNA concentration-dependent intensity of the autoradiograph signal from A. The intensity of the protected bands for the miR-16 (pink square) and U6 probes (blue diamond) were plotted against increasing sRNA concentration. Based on this plot, 0.1 μg sRNA was used in C. C Comparing expression of mmu-miR-107 in 129 and 129.MOLF-Chr19 (CSS) tissues. sRNA (0.1 μg) extracted from adult testes of 129 and 129.MOLF-Chr19, testicular tumor tissues from 129.MOLF-Chr19, E13.5 embryos of 129 and 129.MOLF-Chr19, and PN1 testes of 129 and 129.MOLF-Chr19 were hybridized with ^{32}P-labeled miR-107 and U6 probes before separation on acrylamide gels. Protected U6 and miR-107 fragments are indicated. D Quantitation of intensity of protected fragments of the ^{32}P-labeled miR-107 and U6 probes. Densitometric analysis was used to quantitate the bands. The intensity of each miR-107 protected fragment was compared to the U6 protected fragment. For each lane, the average and standard deviation of two experiments are shown

Table 1

DNA oligos to generate the RPA probes

mmu-mir-101b	5′-TACAGTACTGTGATAGCTGAAGCCTGTCTC
mmu-mir-107	5′-AGCAGCATTGTACAGGGCTATCACCTGTCTC
mmu-mir-192	5′-CTGACCTATGAATTGACACCTGTCTC
mmu-mir-194-2	5′-TGTAACAGCAACTCCATGTGGACCTGTCTC
mmu-mir-204	5′-TTCCCTTTGTCATCCTATGCCTGCCTGTCTC
mmu-mir-146b	5′-TGAGAACTGAATTCCATAGGCTCCTGTCTC
mmu-mir-290	5′-CTCAAACTATGGGGGCACTTTTTCCTGTCTC
mmu-mir-294	5′-AAAGTGCTTCCCTTTTGTGTGTCCTGTCTC
mmu-mir-295	5′-AAAGTGCTACTACTTTTGAGTCTCCTGTCTC
U6 (internal control)	5′-GTGCTCGCTTCGGCAGCACATATACTAAAATTGGAACGATACAGAGAAG ATTAGCATGGCCCCTGCGCAAGGATGACACGCAAATTCGTCCTGTCTC

Table 2

Fold changes in microarray and qRT-PCR

Genes	Fold change (129.MOLF-Chr19 / 129)					
	E13.5 genital ridges		E13.5 embryos		PN1 testes	
	array	qRT-PCR[a]	array	qRT-PCR[a]	array	qRT-PCR[a]
Zfp162	-6.99	-2.89	-8.00	-8.34	-5.39	-15.37
D19Bwg1357e	-5.27	-2.42	-4.47	-1.63	-3.05	-1.72
Cox15	-4.05	-1.29	-5.69	-1.53	-3.79	-1.62

[a]qRT-PCR fold changes are averages of at least two experiments using the same and/or different RNA samples as microarray.